Ecological Indicators 153 (2023) 110448

Contents lists available at ScienceDirect

Ecological Indicators

journal homepage: www.elsevier.com/locate/ecolind

Original Articles

Spatial heterogeneity of vegetation phenology caused by urbanization in China based on remote sensing

Yuan Chen [a], Meixia Lin [a,b], Tao Lin [a,b,*], Junmao Zhang [a,c], Laurence Jones [d], Xia Yao [e], Hongkai Geng [a,c], Yuqin Liu [a,b], Guoqin Zhang [a,b], Xin Cao [a,b,c], Hong Ye [a,b], Yulin Zhan [c,f]

[a] Key Laboratory of Urban Environment and Health, Institute of Urban Environment, Chinese Academy of Sciences, Xiamen 361021, China
[b] Xiamen Key Laboratory of Smart Management on the Urban Environment, Xiamen 361021, China
[c] University of Chinese Academy of Sciences, Beijing 100049, China
[d] Environment Centre Wales, Centre for Ecology & Hydrology, Bangor LL57 2UW, UK
[e] Technical University of Munich, Terrestrial Ecology Research Group, Department of Life Science Systems, School of Life Sciences, Freising 85354, Germany
[f] Aerospace Information Research Institute, Chinese Academy of Sciences, Beijing 100094, China

ARTICLE INFO

Keywords:
Vegetation phenology
Urbanization
Spatial heterogeneity
Vegetation zones
Remote sensing
China

ABSTRACT

Vegetation phenology changes caused by urbanization could lead to shifts in ecosystem services in urban areas and impact on human health. The characteristics of urbanization affect vegetation phenology need to be emphasized, especially in China with a complex natural environment and rapid urbanization background. In this study, we used remote sensing-based phenological data (MODIS MCD12Q2) to analyze the spatial heterogeneity of vegetation phenology caused by urbanization between urban and non-urban areas in 320 cities across China. We found a significant difference between vegetation phenology in urban and its corresponding non-urban area at national and the regional scale. For national scale, the start of the growing season (SOS) was significantly advanced by 2.53 days ($P < 0.001$), and the end of the growing season (EOS) was significantly delayed by 6.72 days ($P < 0.001$), resulting in the growing season length (GSL) was significantly extended by 9.25 days ($P < 0.001$). For regional scale, the changes of SOS, EOS, and GSL caused by urbanization varied from seven vegetation zones in China. As expected for the Tropical monsoon rain forest and rain forest zone (TR) and Tibetan plateau alpine vegetation zone (TP), and Warm-temperate broadleaf deciduous forest zone (WTB), vegetation phenology in other four vegetation zones shows significant differences between urban and non-urban areas. Furthermore, the potential factors driving phenological changes through urbanization were discussed, which will be of great help in understanding the urban ecological process in future studies.

1. Introduction

Vegetation phenology, the timing of seasonal or life cycle events, is a natural phenomenon in which vegetation generates periodic changes due to the influence of surrounding environmental factors, such as temperature, light, and precipitation (Chen et al., 2000; Farnsworth et al., 1995; Liu et al., 2016; White et al., 2002). Phenological changes can reflect the response and adaptation process of vegetation life cycles to changes in the natural environment (Badeck et al., 2004; Fu et al., 2015; Peñuelas et al., 2009; Piao et al., 2007). As such, it is an important indicator reflecting vegetation dynamics as well as a highly sensitive indicator of the impact of climate change (Chuine et al., 2004; Fu et al., 2015; Shen et al., 2018; White et al., 1997), and also represent the spatiotemporal trends of regional ecosystems (Chen and Yu, 2007; Schwartz and Mark, 1992). Satellite-remote sensing to monitor the seasonal and interannual dynamics of vegetation in a wide range of studies (Justice et al., 1985; Moody and Johnson, 2001; Zhang et al., 2006; Zhang et al., 2003). Compared with traditional phenological observations, remote sensing-based phenology data are effective in continuously capturing the spatial pattern of phenological information over large areas (Baret and Guyot, 1991; Zeng et al., 2020; Zhang, 2018; Zhang et al., 2003).

With the use of remote sensing technology, phenological studies in natural ecosystems have been extensively explored (Josep et al., 2009; Richardson et al., 2013), however, studies of urbanization (human activities) impacts on vegetation phenology are limited (Jochner and

* Corresponding author at: Institute of Urban Environment, Chinese Academy of Sciences, 1799 JimeiRoad, Xiamen 361021, China.
E-mail address: tlin@iue.ac.cn (T. Lin).

https://doi.org/10.1016/j.ecolind.2023.110448
Received 30 December 2022; Received in revised form 10 May 2023; Accepted 29 May 2023
Available online 6 June 2023

Menzel, 2015; Li et al., 2017a; Neil and Wu, 2006). Urbanization gradually modifies the urban landscape and its ecology, largely resulting from impervious surfaces replacing vegetated and cropland surfaces (Weng et al., 2009; Weng and Lu, 2008). The resulting urban heat island (UHI) effects have the potential to reshape the vegetation phenological distribution patterns and responses in the urban and its surrounding area (Perreault and Laforest-Lapointe, 2022; Pretzsch et al., 2017). Several studies have reported that vegetation phenology is significantly related to urbanization which has become a major driver in changing the earth's surface (GAZAL et al., 2008; Han and Xu, 2013; Luo et al., 2007; Neil and Wu, 2006; Qiu et al., 2017). However, these phenological differences may vary in different spatial regions or depending on the degree of urbanization. Previous studies have mostly focused on local areas or individual cities (Jochner and Menzel, 2015; Li et al., 2017a), and quantitative research on larger spatial scales is lacking. In addition, the relationships between UHI intensity and the phenological changes of urban vegetation are still inconclusive (Zhou et al., 2016b). Therefore, it is necessary to understand further the spatial relationship between vegetation phenology change and urbanization, and the extent to which its heterogeneity varies under diverse background climates.

As the largest rapidly industrializing country in the world, China has experienced the fastest urbanization in past decades and this trend is expected to continue in upcoming decades (Fent, 2008; Guan et al., 2018; Tan et al., 2016). With the rapid growth and expansion of Chinese cities, there are many suitable research examples for in-depth researches of urbanization-induced changes to vegetation phenology (Zhao et al., 2014; Zhou et al., 2016b). At the same time, the large differences in latitude and climate, elevation and local topography across China will lead to substantial differences in both vegetation types and phenological periods (Piao et al., 2006; Richardson et al., 2013). Given the complexity of the natural environment and its rapid urbanization mentioned above, China is an ideal area to study the phenological characteristics of vegetation affected by urbanization. Existing studies on the relationship between urbanization and vegetation phenology in China have tended to be limited to specific regions or cities (Jochner and Menzel, 2015). For example, some researchers have explored urban vegetation phenology in the middle temperate zone of China (Liang et al., 2016), the Yangtze Delta (Ding et al., 2020; Han and Xu, 2013), the Dongting Lake Basin (Li et al., 2021), Northeast China (Yao et al., 2017), and the cities such as Beijing (Zhang et al., 2022) and Shanghai (Qiu et al., 2017). Other studies have focused on cities with high urbanization intensity. For example, Zhou et al. analyzed the trend of vegetation phenology in 32 major cities distributed across China (Zhou et al., 2016b). Nevertheless, a comprehensive assessment of the impacts of urbanization on phenology across all of China's major cities is still lacking, particularly a comparison across climate types, and urban intensities.

Here, we used continuous remote sensing data obtained from the Moderate Resolution Imaging Spectroradiometer (MODIS) to assess the spatial heterogeneity of vegetation phenology caused by urbanization, and focus on the following questions: (1) does urbanization cause significant differences between vegetation phenology in urban and its corresponding non-urban areas at the national scale in China? If so, (2) is there a spatial heterogeneity of vegetation phenology caused by urbanization in different vegetation zones in China?

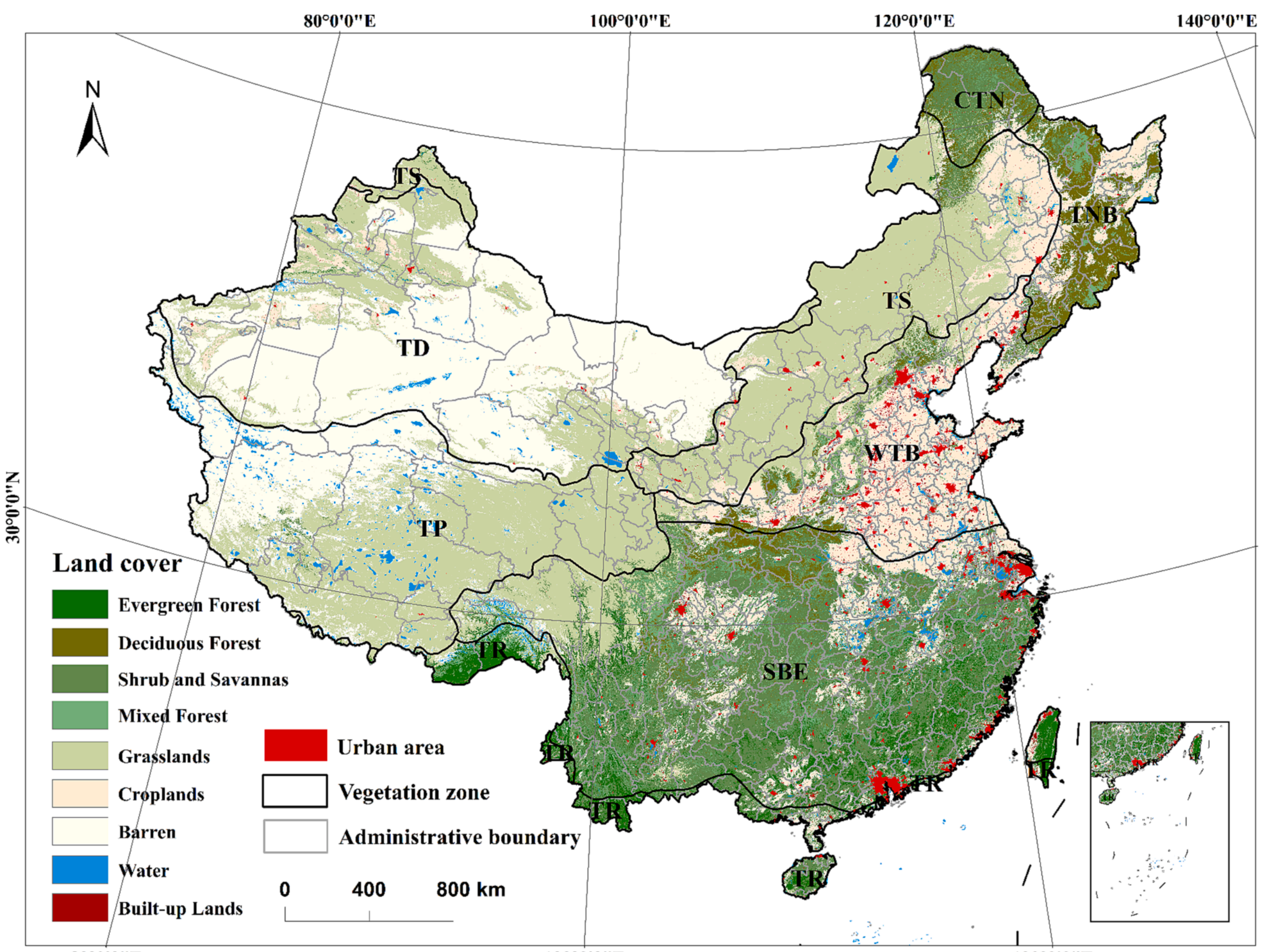

Fig. 1. Locations of the 320 urban areas and eight vegetation regions in China. The land cover map was based on MODIS Land Cover Type Product (MCD12Q1) at 500 m resolution in 2019. The urban areas were extracted from the GlobeLand30 dataset. Krasovsky_1940_Albers was used as the projection coordinate system.

2. Materials and methods

2.1. Study area

In this study, taking the whole territory of China as the study area, the spatial heterogeneity of vegetation phenology caused by urbanization was analyzed at national and regional scales (Fig. 1). China is located in the eastern part of the Eurasian continent and the western Pacific coast (72°-135°E, 19°-55°N), and spans temperature and tropical zones and dry-wet regions. To distinguish the climatic background of different vegetation in China, the land was divided into eight vegetation zones (FANG Jing-Yun and Shi-Long, 2002): Cold-temperate needleleaf forest zone (CTN), Temperate mixed needleleaf and broadleaf deciduous forest zone (TNB), Warm-temperate broadleaf deciduous forest zone (WTB), Subtropical broadleaf evergreen forest zone (SBE), Tropical monsoon rain forest and rain forest zone (TR), Temperate steppe zone (TS), Temperate desert zone (TD), Tibetan plateau alpine vegetation zone (TP).

To spatially represent the urbanization process in China by extracting different scales of urban surfaces, the largest patches of urban areas were selected within each administrative boundary of prefecture-level cities after removing patches smaller than 10 km^2 (Li et al., 2017a). A total of 320 urban areas were selected, with an area ranging from 10.67 km^2 to 9,363.22 km^2, and an average area of 281.33 km^2. The inclusion of cities in each of the Chinese vegetation zones is as follows: 149 cities in SBE zone, 92 cities in WTB zone, 30 cities in TS zone, 20 cities in TD zone, 13 cities in TNB zone, 11 cities in TR zone, 5 cities in TP zone, and no eligible cities in CTN zone.

2.2. Methodology

2.2.1. Extraction of urban and surrounding boundaries

To analyze phenological variation caused by urbanization, it is necessary to delineate the boundaries of urban and its reference areas. Based on the GlobeLand30 dataset in 2020, urban across China was defined by the following steps: (1) to match the pixel size of vegetation phenology data of MODIS (500 m resolution), an urban intensity map which is higher than 50% was generated from the artificial surfaces layer (30 m resolution) using a 1 km × 1 km moving window method (Zhou et al., 2014; Zhou et al., 2016b; Zhou et al., 2015); (2) urban areas were reconstructed with an aggregation distance of 2 km, two times the spatial resolution of the moving window, to aggregate scattered and nearest adjacent built-up patches (Liu et al., 2021); (3) after removing built-up patches smaller than 10 km^2, the largest patches of urban areas were selected within each administrative boundary of prefecture-level cities, which take out the relatively small or densely distributed patches and is still sufficient to cover the numerous cities of development-level of urbanization in China.

Existing studies reported that the urban–rural fringe (the suburbs) has a distinct influence with respect to urbanization. Therefore, neglecting the footprint of the urban–rural fringe may lead to underestimating the impacts of urbanization on phenology (Liu et al., 2021; Zhou et al., 2016b; Zhou et al., 2015). Following previous studies (Zhang et al., 2004; Zhou et al., 2015), we tested the average extent of urbanization effects on vegetation phenology by delineating multiple ring buffers, each of the same size as their associated urban areas. As shown in Fig. 2, the mean phenological differences for the three phenological indicators (see section 2.2.2) leveled off at buffer 4, which the critical areas with the significant and detectable effect by urbanization. Therefore, in this study, the areas affected by urbanization (i.e., urban-affected areas) were excluded, and buffer 4 areas were chosen as non-urban areas to reflect the background or baseline reference phenology for each urban area. For consistency, we finally used the same urban area and non-urban area to calculate the differences of three phenological indicators.

Fig. 3 provides the boundaries for the urban area, the urban-affected area, and the non-urban area, using the Liwan District of Guangzhou city as an example. A mean statistic is calculated for each urban and non-urban area based on the pixel values from remote sensing-based phenology indicators.

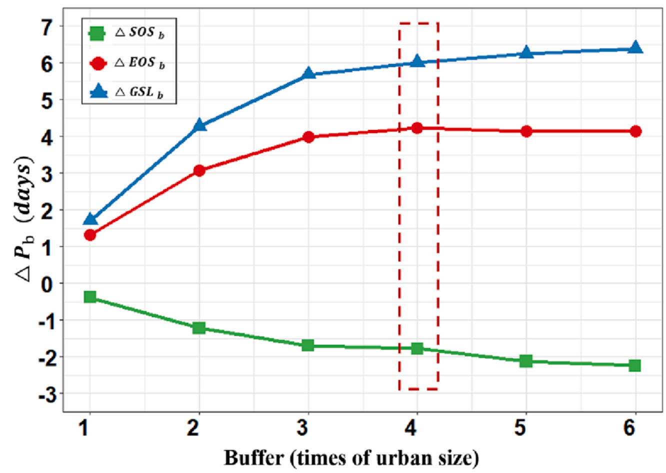

Fig. 2. The trends of average phenological differences from buffer 1 to 6 for 320 areas across China. Buffers 1 to 6 represented the distance away from urban areas. $\triangle P_b$ (i.e., $\triangle SOS_b$, $\triangle EOS_b$, $\triangle GSL_b$) was defined as the phenological differences between urban areas and each buffer.

2.2.2. Vegetation phenology indicators

The vegetation phenology indicators were derived from MODIS Land Cover Dynamic Yearly product (MCD12Q2). To avoid possible outliers due to the selection of individual years, we have extracted remotely sensed vegetation phenological information for a total of six years from 2014 to 2019, with a spatial resolution of 500 m and a temporal resolution of years. For each vegetation transition dates were identified by the extreme points of its curvature value change using a segmented logistifunctionon that was fit to the MODIS two-band Enhanced Vegetation Index (EVI2) as the data source for a given year.

We focused on three remote sensing-based phenology indicators: the start of the growing season (SOS), the end of the growing season (EOS), and the growing season length (GSL). The SOS and EOS correspond to the number of dates from the vegetation transition dates to January 1 of the current year, and the GSL corresponds to the duration between EOS and SOS in the current year. The MCD12Q2 dataset defines the data when EVI2 first crossed 15% of the segment EVI2 amplitude as Greenup and the date when EVI2 last crossed 15% of the segment EVI2 amplitude as Dormancy, which corresponds the pixel values of SOS and EOS, respectively. The pixel values of GSL were calculated by subtracting SOS from EOS. For each pixel, the mean value of the sequence from 2014 to 2019 was calculated to avoid possible errors due to the selection of individual years (Li et al., 2017a). To reduce the uncertainties in vegetation phenology information due to the complexity of the urban landscape, we excluded extreme pixels in remote sensing-phenology data according to previous studies (Li et al., 2017a; Ren et al., 2018; Zhang et al., 2022) and the phenological characteristics of China. Pixels with SOS earlier than the 30th day of the year or later than the 180th day of the year were excluded. Similarly, EOS was constrained to the 150th and 350th of the year.

Further, considering the significant impacts of land cover types on the phenology, especially for rapid urbanization areas in China could increase uncertainties in detecting phenophases accurately. MODIS land cover types data (MCD12Q1) were selected from the same archive with vegetation phenology information for land cover change time series analysis. Finally, about 8% of phenological pixels in which the land cover types were inconsistent during the study period (2014–2019) were excluded and assigned as no data.

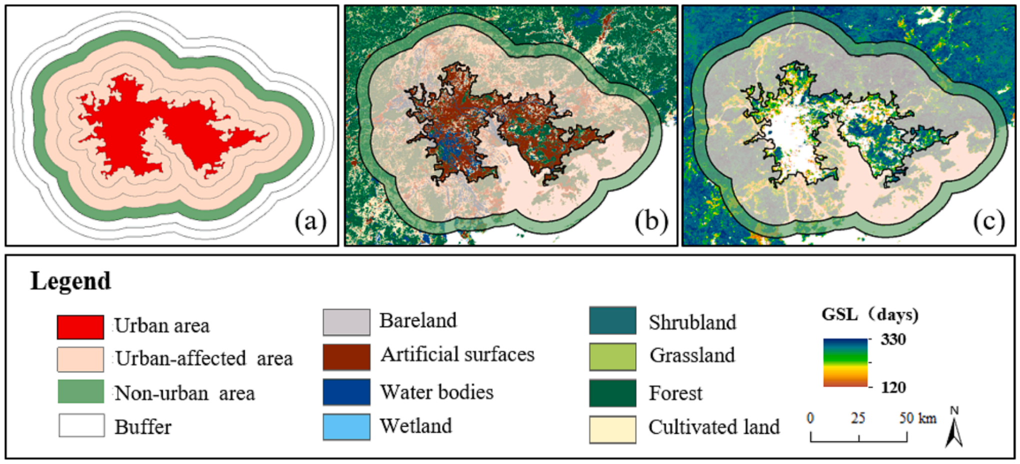

Fig. 3. The delineation of urban and non-urban areas, an example of Liwan District, Guangzhou city. The boundaries of different areas (a). The base map was a land-use map from GlobeLand30 with a spatial resolution of 30 m (b) and a vegetation phenology (GSL) map with a spatial resolution of 500 m (c).

The SOS, EOS, and GSL for each year during 2014–2019 were extracted to calculate annual averages to obtain three phenological information across China. The spatial patterns of vegetation phenology in China was shown in Fig. 4.

In this study, we hypothesized that urban phenology differences relative to non-urban areas are caused by urbanization. $\triangle P$ was calculated as the differences in vegetation phenology between urban and its corresponding non-urban areas for each city (Eq. (1)).

$$\Delta P = P_{ub} - P_{nub} \quad (1)$$

where $\triangle P$ is the difference for each of the three phenology indicators, i.e., $\triangle SOS$, $\triangle EOS$, and $\triangle GSL$, in each urban (P_{ub}) and non-urban area (P_{nub}). A negative $\triangle P$ indicates an advance of SOS or EOS and GSL shorter in urban areas, while a positive $\triangle P$ indicates a delay of SOS or EOS and GSL longer in urban areas.

2.2.3. Statistical analysis

To explore the spatial variations of vegetation phenology caused by urbanization in China, we quantified the differences in three phenology indicators at national and regional scales. Ordinary least-squares (OLS) regression and Paired *t*-test were used to test the relationship between phenological differences in urban areas and non-urban areas. The significance test determined whether the phenological differences were statistically different from zero (i.e., whether the urbanization effect was present), and whether there was a difference in vegetation phenology across regions (Zhou et al., 2016b). In this study, the remote sensing data were pre-processed in MODIS Reprojection Tool, the spatial analysis was completed in ArcGIS 10.7, and the statistical analysis and significance test was implemented in R 4.2.2.

2.3. Datasets

Multi-source remote sensing data and the division map of China were used in this study. First, the urban patches in 2020 were extracted on Artificial Surfaces from the GlobeLand 30 (https://www.globallandcover.com/) with a spatial resolution of 30 m to identify the internal landscape of urban areas more accurately (Chen et al., 2017; Shi et al., 2016). Second, the 349 prefecture-level administrative divisions were obtained from the national basic geographic information databases in 2021 to select the largest urban built-up patches (https://www.webmap.cn/commres.do?method=result100W). Third, the remote sensing-based vegetation phenology over 2014–2019 was derived from the MODIS Land Cover Dynamic Yearly product (MCD12Q2) at 500 m spatial resolution (https://search.earthdata.nasa.gov/) (Ganguly et al., 2010; Gray et al., 2019), which can estimate phenological transition dates on a global scale and has been validated in field observations and used for regional studies (Li et al., 2017a; Yang et al., 2022; Zhang et al., 2022; Zhang et al., 2004). Fourth, the land cover types data was derived

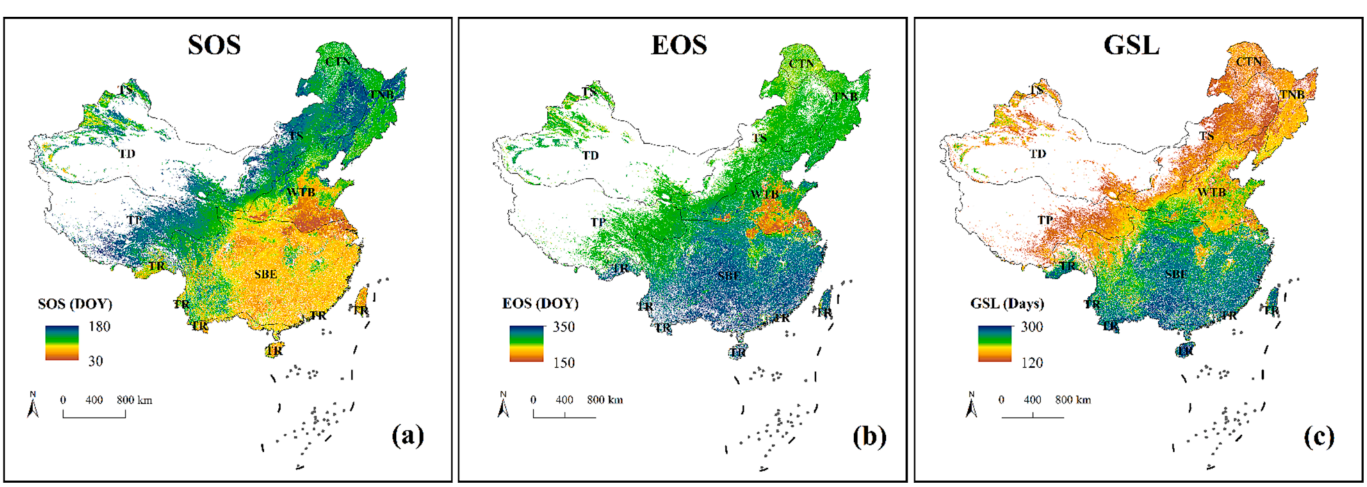

Fig. 4. Spatial patterns of the average vegetation phenology in China over 2014–2019. The spatial mapping of SOS (a), EOS (b), and GSL (c). The empty areas were assigned with no data, which represents the data gaps that are missing due to some reasons e.g., cloud cover or no vegetation, or several pixels that are excluded.

from MODIS Land Cover data (MCD12Q1) over the same period with phenological informations. (https://search.earthdata.nasa.gov/search/). Fifth, Chinese vegetation zones were provided by the Resources and Environmental Sciences and Date Center, Chinese Academy of Sciences (https://www.resdc.cn/data.aspx?DATAID=133). The study area was divided into eight vegetation zones: Cold-temperate needleleaf forest zone (CTN), Temperate mixed needleleaf and broadleaf deciduous forest zone (TNB), Warm-temperate broadleaf deciduous forest zone (WTB), Subtropical broadleaf evergreen forest zone (SBE), Tropical monsoon rain forest and rain forest zone (TR), Temperate steppe zone (TS), Temperate desert zone (TD), Tibetan plateau alpine vegetation zone (TP).

3. Results

3.1. Vegetation phenology variation caused by urbanization at the national scale in China

At the national scale, there were statistically significant differences ($P < 0.001$) between urban and non-urban areas for all three phenology indicators (i.e., SOS, EOS, and GSL) across the 320 urban areas in China (Table 1).

The start of the growing season (SOS) was significantly advanced by 2.53 days in urban areas (t = -2.53, $P < 0.001$), with the average SOS in urban areas of 102.34 DOY (i.e., in mid-April), while that of non-urban areas was 104.88 DOY. This average masks considerable regional differences. As shown in Fig. 5(b), the SOS exhibited a trend of advance in 214 out of 320 urban areas, with the largest advance of 22.9 days in Lianyun District, WTB zone. However, the SOS was delayed in 106 urban areas, mainly in TD zone and SBE zone, and only six cities were delayed by more than 15 days, with the largest delay of 30.4 days in Duzishan District, TD zone.

The end of the growing season (EOS) was significantly delayed in urban areas by 6.72 days on average (t = 6.72, $P < 0.001$), with the average EOS in urban areas of 297.15 DOY (i.e., in late October), compared with that of non-urban areas of 290.43 DOY. As with SOS, this average masks considerable regional differences in EOS. As shown in Fig. 5(d), the EOS showed a delay in 237 out of 320 urban areas, with 37 urban areas delayed by 25 days or more, mainly in the SBE zone, with the largest delay of 55.51 days in Youjiang District, SBE zone. Conversely, the EOS was advanced in 83 urban areas, with the largest advance of 54.80 days in the Lianyun District, WTB zone.

With changes in SOS and EOS, the growing season length (GSL) was also altered. GSL was significantly extended in urban areas (t = 9.25, $P < 0.001$), the average GSL in urban areas was 197.01 days, longer than the 187.77 days in non-urban areas. Consequently, GSL was extended on average by 9.25 days in urban areas. The average masks considerable differences between regions. As shown in Fig. 5(f), the GSL was longer in 226 out of 320 urban areas, with 59 urban areas showing a longer GSL than 25 days, mainly in the SBE zone and TR zone. The longest extension to GSL was 63.72 days in Youjiang District, SBE zone. However, the GSL was shorter in 94 urban areas, with the greatest advancement being 39.62 days in Duzishan District, TD zone.

3.2. Variation in vegetation phenology due to urbanization in different vegetation zones in China

At the regional scale, there was spatial heterogeneity of vegetation phenology changes caused by urbanization varies across the seven vegetation zones (Table 2).

SOS differences (i.e., △SOS) were significant ($P \leq 0.01$) in three vegetation zones across China (Fig. 6), including SBE zone, TD zone, and TNB zone, while no significant differences were found in the other four zones. Specifically, the average SOS in SBE zone and TNB zone was advanced by 2.67 days ($P \leq 0.05$) and 6.21 days ($P \leq 0.001$), respectively. By contrast, the average SOS in TD zone showed the largest delay with an average of 9.46 days ($P \leq 0.001$), with 18 out of 20 cities having a delayed SOS in urban areas.

EOS differences (i.e., △EOS) were significant (P ≤ 0.05) in three vegetation zones across China (Fig. 7), including SBE zone, TR zone, and TNB zone, while no significant differences were found in the other four zones. Specifically, the average EOS in SBE zone showed the largest delay with an average of 13.42 days (P ≤ 0.001), with 128 out of 149 cities having a delayed EOS in urban areas. The average EOS in TNB zone was delayed by 4.82 days (P ≤ 0.05). By contrast, the average EOS in TR zone was advanced by 0.96 days (P ≤ 0.001), with 8 out of 11 cities having an advanced EOS in urban areas.

GSL differences (i.e., △GSL) were significant (P ≤ 0.05) in three vegetation zones across China (Fig. 8), while no significant differences were found in the other four zones. Specifically, the average GSL in SBE zone showed the largest extension with an average of 16.38 days (P ≤ 0.001), with 125 out of 149 cities having a delayed EOS in urban areas. The average GSL in TNB zone was extended by 11.27 days (P ≤ 0.05). By contrast, the average GSL in TR zone was shortened by 5.07 days (P ≤ 0.001), and all urban areas in this zone had a shorten GSL.

4. Discussion

4.1. Spatial heterogeneity of vegetation phenology caused by urbanization in China

By contrasting vegetation phenology in urban and non-urban areas, we demonstrate a statistically significant difference in vegetation phenology across China and have quantified vegetation phenology changes caused by urbanization. The predominant effect was that the phenological cycle in urban areas started earlier and ended later, and the growing season length was longer, consistent with previous findings in the conterminous United States (Li et al., 2017a; Meng et al., 2020) and China (Ren et al., 2018). However, we found that both the direction and magnitude of phenological change varied in different vegetation zones in China. For example, the TD zone showed an opposite change pattern as that of the national scale, where the phenological cycle started later (△SOS = 9.46) and ended earlier (△EOS = -6.38), resulting in a shorter growing season length. These opposite change patterns in some urban areas might be attributed to their heterogeneous local conditions (Li et al., 2017a). In our study, the spatial heterogeneity of vegetation phenology changes caused by urbanization varies across different zones and was confirmed by the division of vegetation zones in China.

Table 1
Comparison of average vegetation phenology in urban and non-urban areas ($n = 320$), across all climate zones.

	SOS (DOY)			EOS (DOY)			GSL(Days)		
	U-SOS	NU-SOS	△SOS	U-EOS	NU-EOS	△EOS	U-GSL	NU-GSL	△GSL
Max	163.14	160.46	30.36	345.47	327.91	55.51	264.31	245.43	63.72
Min	48.74	61.54	−22.92	202.75	220.39	−54.80	125.40	129.17	−39.62
Mean	102.34	104.88	−2.53	297.15	290.43	6.72	197.01	187.77	9.25
Std	28.12	25.46	8.23	28.22	17.96	15.35	39.32	30.63	16.60
t-test	−2.53***			6.72***			9.25***		

Note: DOY refers to the growing date of the year; Days refers to the growing days of the year; ****t*-test results are Significant at the 0.001 level.

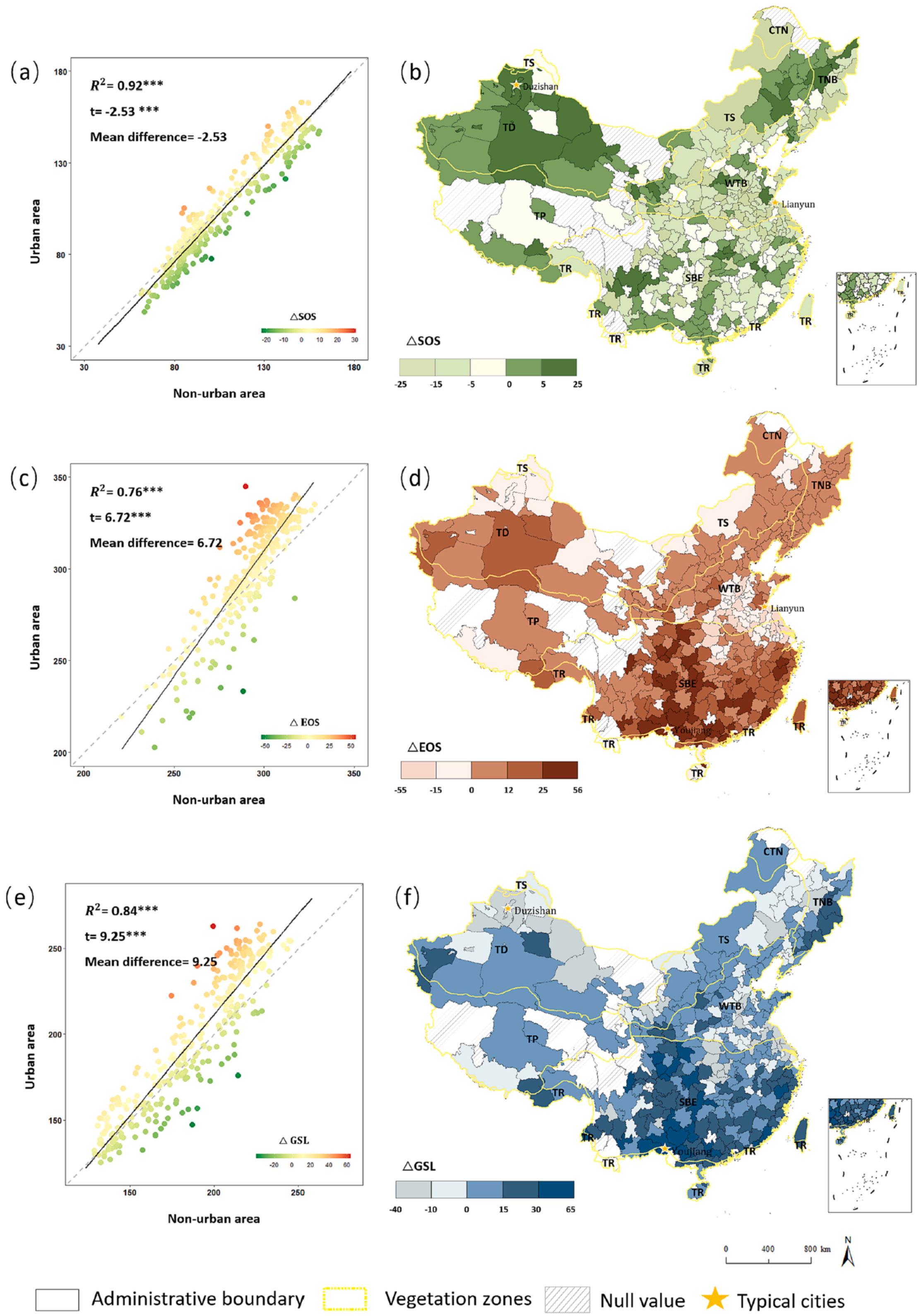

Fig. 5. Comparison of the three phenology indicators between urban and non-urban areas at the national scale. The scatter shows the relationship between urban and non-urban areas in SOS (a), EOS (c), and GSL (e); Gradient red points show that SOS or EOS is later or GSL is longer in the urban area; gradient green points show that SOS or EOS is earlier or GSL shorter in the urban area. The gray dotted line indicates the 1:1 line, and the black solid line indicates the linear regression. The spatial distribution mapping shows the difference between urban and non-urban areas in SOS (b), EOS (d), and GSL (f), by region. The dark colors indicate SOS or EOS is later or GSL is longer in the urban area; the light colors indicate SOS or EOS is earlier or GSL shorter in the urban area. Note: *** indicates the results are significant at 0.001 level. (For interpretation of the references to colour in this figure legend, the reader is referred to the web version of this article.)

Table 2
Comparison of phenological differences in seven vegetation zones.

	△SOS (days)				△EOS (days)				△GSL (days)			
	Max	Min	Mean	Std	Max	Min	Mean	Std	Max	Min	Mean	Std
TNB (*n* = 13)	13.80	−20.34	−6.21	10.07	7.55	−2.45	4.82	2.74	22.58	−6.03	11.03	10.13
WTB (*n* = 92)	14.22	−22.92	−6.13	7.31	22.82	−54.80	−2.45	14.13	29.47	−32.92	3.68	11.90
SBE (*n* = 149)	20.24	−18.37	−2.67	6.49	55.51	−33.97	13.42	15.53	63.72	−38.26	16.09	16.76
TP (*n* = 5).	13.19	−2.31	5.48	5.99	20.63	−6.11	8.66	8.62	25.98	−9.04	3.18	12.79
TR (*n* = 11)	9.31	−12.02	−2.02	7.28	30.31	−31.41	−0.96	17.40	13.49	−29.64	1.06	13.58
TS (*n* = 30)	18.33	−13.36	1.27	8.87	27.12	−9.13	14.12	12.96	41.71	2.00	12.85	12.07
TD (*n* = 20)	30.36	−0.87	9.46	24.48	−11.42	3.65	−6.38	9.94	18.48	−39.62	−15.84	14.63

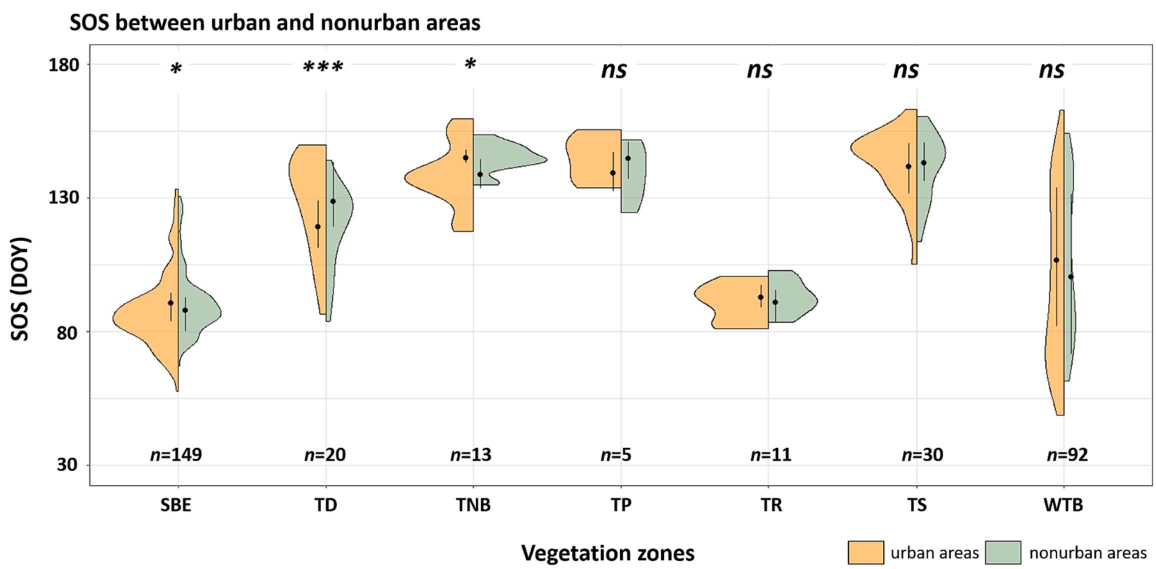

Fig. 6. SOS at different vegetation zones in urban and non-urban areas. Note: ns indicates the results are nonsignificant, **indicates the results are significant at the 0.01 level, *** indicates the results are significant at the 0.001 level; n indicates the number of area samples for each zone.

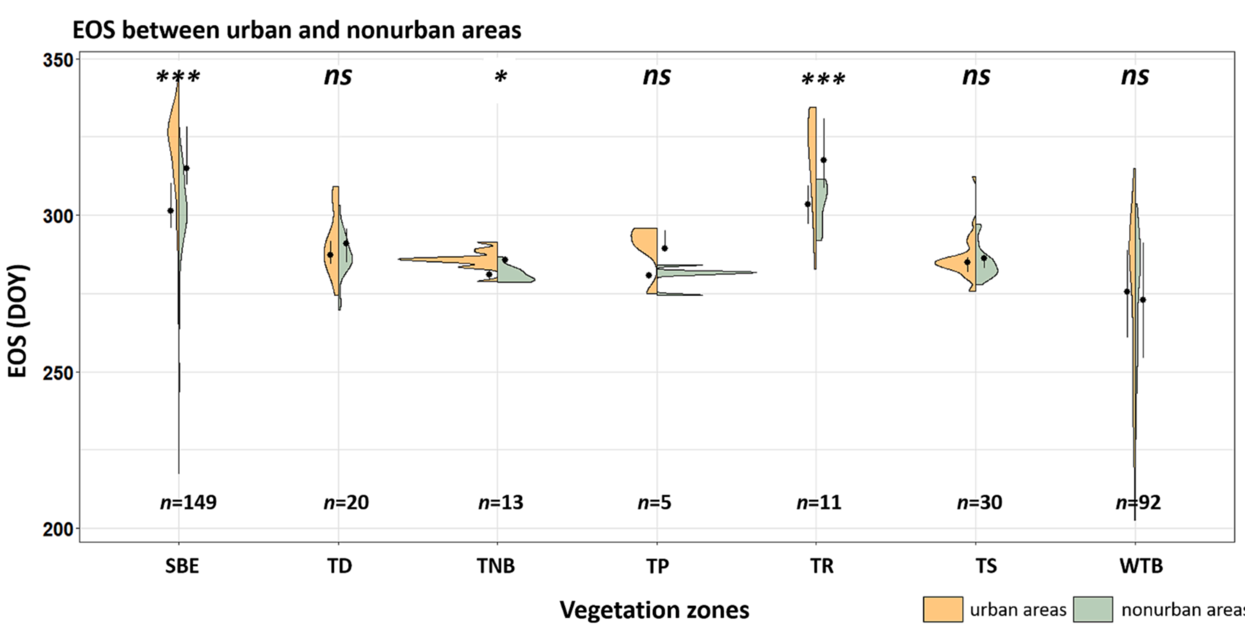

Fig. 7. EOS at different vegetation zones in urban and non-urban areas. Note: ns indicates the results are nonsignificant, *** indicates the results are significant at the 0.001 level; n indicates the number of area samples for each zone.

Specifically, none of the phenological indicators in the TS zone, WTB zone, and the TP zone showed significant differences ($P > 0.05$) between urban and non-urban areas, which may be related to the zones-specific growing conditions and physiological characteristics of the species (Jochner and Menzel, 2015). In addition, when we excluded areas with inconsistent land cover due to rapid urbanization during the study

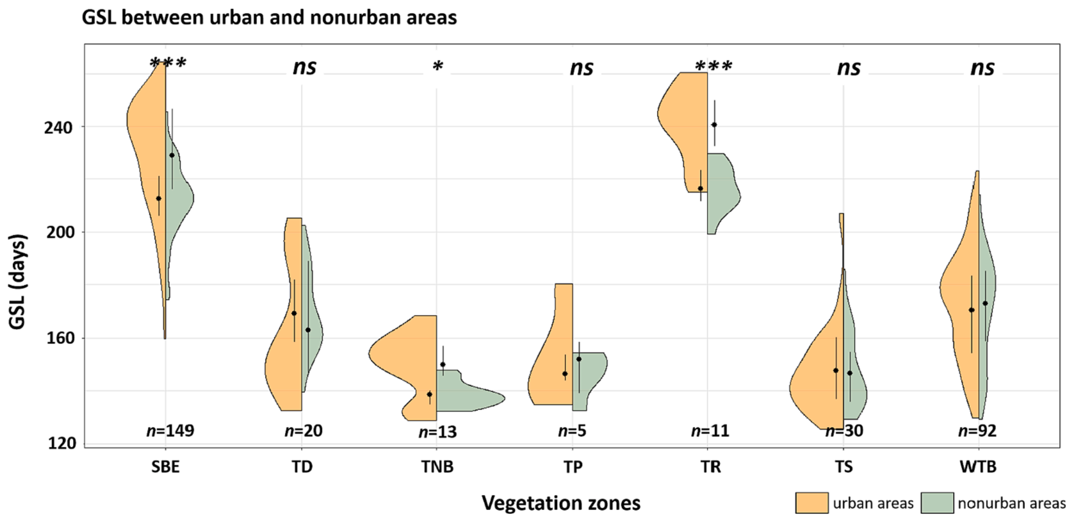

Fig. 8. GSL at different vegetation zones in urban and non-urban areas. Note: ns indicates the results are nonsignificant, * indicates the results are significant at the 0.05 level, **indicates the results are significant at the 0.01 level, *** indicates the results are significant at the 0.001 level; n indicates the number of area samples for each zone.

period, the WTB zones with higher urban density and more extensive arable land showed no significance differences, which may be related to land cover noise. The land cover change should not be ignored in detections of the differences in phenology between urban and non-urban areas, considering the rapid urbanization in China and the significant impacts of land cover types on the phenology. Furthermore, the significance of phenological differences in the same zone varied for three phenological indicators, possibly indicating that each vegetation growth period was controlled by distinct factors (Zhou et al., 2016b).

4.2. Potential driving factors of urbanization on vegetation phenology in China

Urbanization may increase or inhibit vegetation growth, thereby impacting vegetation phenology. The effect of urbanization on vegetation phenology and its spatial changes can be attributed to many confounding factors. Previous studies have shown that temperature explains more than two-thirds of the variation in phenological start dates (Jochner and Menzel, 2015; Menzel and Fabian, 1999). Studies have reported that urban warming advances the start of the growing season (SOS) (Meng et al., 2020) and leads to shorter vegetation growing seasons (GSL) (Kabano et al., 2021). The difference between surface temperature in urban and rural areas (i.e., urban heat island intensity) was significantly correlated with the urban–rural phenology. Meanwhile, some sampling experiments or remote sensing observations have reported that exposure to the presence of aerosols and air pollutants has adverse effects on vegetation phenology (Honour et al., 2009). In addition to the impacts of anthropogenic activities, changes in the natural surface caused by urbanization in specific cities can also alter local microclimate conditions, which act as an important factor in vegetation phenology changes (D'odorico et al., 2013; Robitu et al., 2006). The replacement of vegetation for impervious surfaces may promote the creation of an urban microclimate through a variety of processes (Duarte et al., 2015), such as more sensible heat flux (Avissar and Mahrer, 1982), lack of daylight (Sternberg et al., 2011) as well as changes in humidity (Kottner et al., 2018) in urban canyons and near-surface atmospheres. Altering energy balance can indeed influence urban phenological behavior at the local scale. However, Buyantuyev and Wu (Buyantuyev and Wu, 2012) found a complex phenology change that is not synchronized with climate variability, providing evidence that socioeconomic factors also drive vegetation phenology changes. For example, increasing population pressures (Li et al., 2019), Gross Domestic Product growth (Zhang et al., 2021), and livestock density (Venkatesh et al., 2022) are often associated with vegetation phenology changes in specific regions. Furthermore, differences in vegetation phenology between urban and the surrounding area may also be caused by the diversity of the vegetation types (Li et al., 2017a). Urbanization can strongly alter phenological characteristics through urban greening with exotic species and human management practices and is therefore more manipulated by human activities than the natural vegetation in non-urban areas. Overall, vegetation phenology in urban environments appears to be driven by a variety of factors, and these influences may vary in different geographical regions. At present, detailed investigations of the driving mechanism of vegetation phenological differences caused by urbanization have not been explored through the coupling of climate variability and socioeconomic trends in the urbanization process, which is a knowledge gap that should be addressed.

4.3. Limitations and uncertainties

There are some limitations in this study. Firstly, cropland was not excluded from our study since most cities are mainly surrounded by agricultural land during the urbanization process in China (Zhou et al., 2016a). While the phenology of cropland is usually affected by crop type and human management (Buyantuyev and Wu, 2012; Zhou et al., 2016b), resulting in uncertainties from cropland-phenological values in non-urban areas. Secondly, although MCD12Q2 datasets have been widely used for urban phenology studies, results derived from these relatively coarse spatial resolution datasets may not be suitable to capture vegetation phenological information in heterogeneous urban surfaces with sparse and highly mixed vegetation coverage (Li et al., 2017b; Sohl et al., 2007; Yu et al., 2014). Thirdly, our study focuses on the differences in vegetation phenology changes at large scales and thus neglected the species-specific detail for each area, which may result in some uncertainties (Li et al., 2019; Li et al., 2017a). It might be necessary to further combine high-resolution satellite data and ground observations to provide more detailed spatial information in the urban environment.

5. Conclusions

Our study provided a quantitative analysis of the spatial heterogeneity of urbanization-induced vegetation phenology in 320 urban areas across China at a national and vegetation zones scales, using three phenological indicators derived from continuous remote sensing data (MODIS MCD12Q2). At the national scale, the vegetation phenology had a statistically significant difference between urban and its corresponding non-urban areas: the SOS was significantly advanced by an averaged of 1.95 days, while the EOS was significantly delayed by 4.49 days in urban areas. The GSL was significantly extended by 6.44 days in urban areas. However, there is a spatial variation in the phenological differences across cities in the different vegetation zones in China. The SOS differences between urban and its corresponding non-urban areas were significant in SBE zone, TD zone, and TS zone. The EOS differences were significant in TNB zone and WTB zone. The GSL differences were significant in five vegetation zones across China, except in the TR and TP zones. Specifically, none of the phenological indicators in TR zone and TP zone showed significant differences. In the future, exploring the spatial and temporal patterns of vegetation phenology and their response mechanisms under regional urbanization factors is needed, to provide scientific and technological support for regional and urban responses to future warming and rational urban green space planning.

CRediT authorship contribution statement

Yuan Chen: Conceptualization, Data curation, Methodology, Investigation, Formal analysis, Writing – original draft, Visualization. **Meixia Lin:** Conceptualization, Methodology, Writing – review & editing. **Tao Lin:** Conceptualization, Methodology, Supervision, Writing – review & editing. **Junmao Zhang:** Methodology, Visualization, Writing – review & editing. **Laurence Jones:** Writing – review & editing. **Xia Yao:** Visualization, Writing – review & editing. **Hongkai Geng:** Writing – review & editing. **Yuqin Liu:** Writing – review & editing. **Guoqin Zhang:** Methodology, Visualization. **Xin Cao:** Visualization. **Hong Ye:** Writing – review & editing. **Yulin Zhan:** Writing – review & editing.

Declaration of Competing Interest

The authors declare that they have no known competing financial interests or personal relationships that could have appeared to influence the work reported in this paper.

Data availability

Data will be made available on request.

Acknowledgments

This work was supported by the Strategic Priority Research Program of the Chinese Academy of Sciences (Grant No.XDA23030104); the Major Special Project-the China High-Resolution Earth Observation System (30-Y30F06-9003-20/22); the International Partnership Program of Chinese Academy of Sciences (Grant No.132C35K-YSB20200007); the National Natural Science Foundation of China (42271299) and Xiamen Key Laboratory of smart management on the urban environment.

References

Avissar, R., Mahrer, Y., 1982. Verification study of a numerical greenhouse microclimate model. 25, 1711-1720.doi: 10.13031/2013.33794.

Badeck, F.W., Bondeau, A., Böttcher, K., Doktor, D., Lucht, W., Schaber, J., Sitch, S., 2004. Responses of spring phenology to climate change. New Phytol. 162, 295–309. https://doi.org/10.1111/j.1469-8137.2004.01059.x.

Baret, F., Guyot, G., 1991. Potentials and limits of vegetation indices for LAI and APAR assessment. Remote Sens. Environ. 35, 161–173. https://doi.org/10.1016/0034-4257(91)90009-U.

Buyantuyev, A., Wu, J., 2012. Urbanization diversifies land surface phenology in arid environments: interactions among vegetation, climatic variation, and land use pattern in the Phoenix metropolitan region, USA. Landsc. Urban Plan. 105, 149–159. https://doi.org/10.1016/j.landurbplan.2011.12.

Chen, J., Cao, X., Peng, S., Ren, H., 2017. Analysis and applications of GlobeLand30: a review. ISPRS Int. J. Geo Inf. 6, 230. https://doi.org/10.3390/ijgi6080230.

Chen, X., Tan, Z., Schwartz, M.D., Xu, C., 2000. Determining the growing season of land vegetation on the basis of plant phenology and satellite data in Northern China. Int. J. Biometeorol. 44, 97–101. https://doi.org/10.1007/s004840000056.

Chen, X.-Q., Yu, R., 2007. Spatial and temporal variations of the vegetation growing season in warm-temperate eastern China during 1982 to 1999. Acta Geographica Sinica-Chin. Ed.- 62, 41.

Chuine, I., Yiou, P., Viovy, N., Seguin, B., Daux, V., Ladurie, E.L.R., 2004. Historical phenology: grape ripening as a past climate indicator. Nature 432, 289–290. https://doi.org/10.1038/432289a.

Ding, H., Xu, L., Elmore, A.J., Shi, Y., 2020. Vegetation phenology influenced by rapid urbanization of The Yangtze Delta region. Remote Sens. (Basel) 12, 1783. https://doi.org/10.3390/rs12111783.

D'odorico, P., He, Y., Collins, S., De Wekker, S.F., Engel, V., Fuentes, J.D.J.G.E., Biogeography, 2013. Vegetation–microclimate feedbacks in woodland–grassland ecotones. 22, 364-379.doi: 10.1111/geb.12000.

Duarte, D.H.S., Shinzato, P., Gusson, C.D.S., Alves, C.A., 2015. The impact of vegetation on urban microclimate to counterbalance built density in a subtropical changing climate. Urban Clim. 14, 224–239.

FANG Jing-Yun, S.Y.-C., LIU Hong-Yan, Shi-Long, P., 2002. Vegetation-climate relationship and its application in the division of vegetation zone in China. J. Integr. Plant Biol., 44, 1105-1122. doi: 10.3321/j.issn:1672-9072.2002.09.009.

Farnsworth, E.J., Nunez-Farfan, J., Careaga, S.A., Bazzaz, F.A., 1995. Phenology and growth of three temperate forest life forms in response to artificial soil warming. J. Ecol. 83, 967–977. https://doi.org/10.2307/2261178.

Fent, T., 2008. Department of economic and social affairs, population division, united nations expert group meeting on social and economic implications of changing population age structures. Eur. J. Popul. 24 (4), 451–452.

Fu, Y.H., Zhao, H., Piao, S., Peaucelle, M., Peng, S., Zhou, G., Ciais, P., Huang, M., Menzel, A., Peñuelas, J., Song, Y., Vitasse, Y., Zeng, Z., Janssens, I.A., 2015. Declining global warming effects on the phenology of spring leaf unfolding. Nature 526 (7571), 104–107.

Ganguly, S., Friedl, M.A., Tan, B., Zhang, X., Verma, M., 2010. Land surface phenology from MODIS: Characterization of the Collection 5 global land cover dynamics product. Remote Sens. Environ. 114, 1805–1816. https://doi.org/10.1016/j.rse.2010.04.005.

Gazal, R., White, M.A., Gillies, R., Rodemaker, E., Sparrow, E., Gordon, L., 2008. GLOBE students, teachers, and scientists demonstrate variable differences between urban and rural leaf phenology. Glob. Chang. Biol. 14, 1568–1580. https://doi.org/10.1111/j.1365-2486.2008.01602.x.

Gray, J., Sulla-Menashe, D., Friedl, M.A., 2019. User guide to collection 6 modis land cover dynamics (mcd12q2) product. NASA EOSDIS Land Processes DAAC: Missoula, MT, USA 6, 1-8.

Guan, X., Wei, H., Lu, S., Dai, Q., Su, H., 2018. Assessment on the urbanization strategy in China: Achievements, challenges and reflections. Habitat Int. 71, 97–109.

Han, G., Xu, J., 2013. Land surface phenology and land surface temperature changes along an urban–rural gradient in Yangtze River Delta, China. Environ. Manag. 52, 234–249. https://doi.org/10.1007/s00267-013-0097-6.

Honour, S.L., Bell, J.N.B., Ashenden, T.W., Cape, J.N., Power, S.A., 2009. Responses of herbaceous plants to urban air pollution: Effects on growth, phenology and leaf surface characteristics. Environ. Pollut. 157, 1279–1286. https://doi.org/10.1016/j.envpol.2008.11.049.

Jochner, S., Menzel, A., 2015. Urban phenological studies–Past, present, future. Environ. Pollut. 203, 250–261. https://doi.org/10.1016/j.envpol.2015.01.003.

Justice, C.O., Townshend, J.R., Holben, B.N., Tucker, C.J., 1985. Analysis of the phenology of global vegetation using meteorological satellite data. Int. J. Remote Sens. 6, 1271–1318. https://doi.org/10.1080/01431168508948281.

Kabano, P., Lindley, S., Harris, A., 2021. Evidence of urban heat island impacts on the vegetation growing season length in a tropical city. Landsc. Urban Plan. 206, 103989 https://doi.org/10.1016/j.landurbplan.2020.103989.

Kottner, J., Black, J., Call, E., Gefen, A., Santamaria, N.J.C.B., 2018. Microclimate: a critical review in the context of pressure ulcer prevention. 59, 62-70.doi: 10.1016/j.clinbiomech.2018.09.010.

Li, D., Stucky, B.J., Deck, J., Baiser, B., Guralnick, R.P., 2019. The effect of urbanization on plant phenology depends on regional temperature. Nat. Ecol. Evol. 3, 1661–1667. https://doi.org/10.1038/s41559-019-1004-1.

Li, P., Sun, M., Liu, Y., Ren, P., Peng, C., Zhou, X., Tang, J., 2021. Response of Vegetation Photosynthetic Phenology to Urbanization in Dongting Lake Basin, China. Remote Sensing 13, 3722. https://doi.org/10.3390/rs13183722.

Li, X., Zhou, Y., Asrar, G.R., Mao, J., Li, X., Li, W., 2017a. Response of vegetation phenology to urbanization in the conterminous United States. Glob. Chang. Biol. 23, 2818–2830. https://doi.org/10.1111/gcb.13562.

Li, X., Zhou, Y., Asrar, G.R., Meng, L., 2017b. Characterizing spatiotemporal dynamics in phenology of urban ecosystems based on Landsat data. Sci. Total Environ. 605–606, 721–734. https://doi.org/10.1016/j.scitotenv.2017.06.245.

Liang, S., Shi, P., Li, H., 2016. Urban spring phenology in the middle temperate zone of China: dynamics and influence factors. Int. J. Biometeorol. 60, 531–544. https://doi.org/10.1007/s00484-015-1049-z.

Liu, Q., Fu, Y.H., Zhu, Z., Liu, Y., Liu, Z., Huang, M., Janssens, I.A., Piao, S., 2016. Delayed autumn phenology in the Northern Hemisphere is related to change in both climate and spring phenology. Glob. Chang. Biol. 22, 3702–3711. https://doi.org/10.1111/gcb.13311.

Liu, H., Huang, B., Zhan, Q., Gao, S., Li, R., Fan, Z., 2021. The influence of urban form on surface urban heat island and its planning implications: Evidence from 1288 urban clusters in China. Sustain. Cities Soc. 71, 102987 https://doi.org/10.1016/j.scs.2021.102987.

Luo, Z., Sun, O.J., Ge, Q., Xu, W., Zheng, J., 2007. Phenological responses of plants to climate change in an urban environment. Ecol. Res. 22, 507–514. https://doi.org/10.1007/s11284-006-0044-6.

Meng, L., Mao, J., Zhou, Y., Richardson, A.D., Lee, X., Thornton, P.E., Ricciuto, D.M., Li, X., Dai, Y., Shi, X., Jia, G., 2020. Urban warming advances spring phenology but reduces the response of phenology to temperature in the conterminous United States. Proc. Natl. Acad. Sci. U.S.A. 117 (8), 4228–4233.

Menzel, A., Fabian, P., 1999. Growing season extended in Europe. Nature 397, 659-659. doi: 10.1038/17709.

Moody, A., Johnson, D.M., 2001. Land-Surface Phenologies from AVHRR Using the Discrete Fourier Transform. Remote Sens. Environ. 75, 305–323. https://doi.org/10.1016/S0034-4257(00)00175-9.

Neil, K., Wu, J., 2006. Effects of urbanization on plant flowering phenology: a review. Urban Ecosystems 9, 243–257. https://doi.org/10.1007/s11252-006-9354-2.

Peñuelas, J., Rutishauser, T., Filella, I., 2009a. Ecology. Science 324 (5929), 887–888.

Peñuelas, J., Rutishauser, T., Filella, I., 2009b. Phenology feedbacks on climate change. Science 324, 887–888. https://doi.org/10.1126/science.1173004.

Perreault, R., Laforest-Lapointe, I., 2022. Plant-microbe interactions in the phyllosphere: facing challenges of the anthropocene. ISME J. 16, 339–345. https://doi.org/10.1038/s41396-021-01109-3.

Piao, S., Fang, J., Zhou, L., Ciais, P., Zhu, B., 2006. Variations in satellite-derived phenology in China's temperate vegetation. Glob. Chang. Biol. 12 (4), 672–685.

Piao, S., Friedlingstein, P., Ciais, P., Viovy, N., Demarty, J., 2007. Growing season extension and its impact on terrestrial carbon cycle in the Northern Hemisphere over the past 2 decades. Global Biogeochem. Cycles 21 (3), n/a–n/a.

Pretzsch, H., Biber, P., Uhl, E., Dahlhausen, J., Schütze, G., Perkins, D., Rötzer, T., Caldentey, J., Koike, T., Con, T.V., Chavanne, A., Toit, B.d., Foster, K., Lefer, B., 2017. Climate change accelerates growth of urban trees in metropolises worldwide. Sci. Rep. 7 (1) https://doi.org/10.1038/s41598-017-14831-w.

Qiu, T., Song, C., Li, J., 2017. Impacts of urbanization on vegetation phenology over the past three decades in Shanghai, China. Remote Sensing 9, 970. https://doi.org/10.3390/rs9090970.

Ren, Q., He, C., Huang, Q., Zhou, Y., 2018. Urbanization impacts on vegetation phenology in China. Remote Sens. (Basel) 10, 1905.

Richardson, A.D., Keenan, T.F., Migliavacca, M., Ryu, Y., Sonnentag, O., Toomey, M., 2013. Climate change, phenology, and phenological control of vegetation feedbacks to the climate system. Agric. For. Meteorol. 169, 156–173. https://doi.org/10.1016/j.agrformet.2012.09.012.

Robitu, M., Musy, M., Inard, C., Groleau, D.J.S.e., 2006. Modeling the influence of vegetation and water pond on urban microclimate. 80, 435-447. doi: 10.1016/j.solener.2005.06.015.

Schwartz, Mark, D., 1992. Phenology and springtime surface-layer change. Mon. Wea. Rev. 120, 2570. https://doi.org/10.1175/1520-0493(1992)1202.0.CO;2.

Shen, X., Liu, B., Henderson, M., Wang, L., Wu, Z., Wu, H., Jiang, M., Lu, X., 2018. Asymmetric effects of daytime and nighttime warming on spring phenology in the temperate grasslands of China. Agric. For. Meteorol. 259, 240–249. https://doi.org/10.1016/j.agrformet.2018.05.006.

Shi, X., Nie, S., Ju, W., Yu, L., 2016. Application and impacts of the GlobeLand30 land cover dataset on the Beijing Climate Center Climate Model. IOP Conference Series: Earth and Environmental Science 34, 012032. https://doi.org/10.1088/1755-1315/34/1/012032.

Sohl, T.L., Sayler, K.L., Drummond, M.A., Loveland, T.R., 2007. The FORE-SCE model: a practical approach for projecting land cover change using scenario-based modeling. J. Land Use Sci. 2, 103–126. https://doi.org/10.1080/17474230701218202.

Sternberg, T., Viles, H., Cathersides, A.J.B., Environment, 2011. Evaluating the role of ivy (Hedera helix) in moderating wall surface microclimates and contributing to the bioprotection of historic buildings. 46, 293-297.doi: 10.1016/j.buildenv.2010.07.017.

Tan, Y., Xu, H., Zhang, X., 2016. Sustainable urbanization in China: a comprehensive literature review. Cities 55, 82–93.

Venkatesh, K., John, R., Chen, J., Jarchow, M., Amirkhiz, R.G., Giannico, V., Saraf, S., Jain, K., Kussainova, M., Yuan, J., 2022. Untangling the impacts of socioeconomic and climatic changes on vegetation greenness and productivity in Kazakhstan. Environ. Res. Lett. 17 (9), 095007.

Weng, Q., Lu, D., 2008. A sub-pixel analysis of urbanization effect on land surface temperature and its interplay with impervious surface and vegetation coverage in Indianapolis, United States. Int. J. Appl. Earth Obs. Geoinf. 10, 68–83. https://doi.org/10.1016/j.jag.2007.05.002.

Weng, Q., Hu, X., Liu, H., 2009. Estimating impervious surfaces using linear spectral mixture analysis with multitemporal ASTER images. Int. J. Remote Sens. 30, 4807–4830. https://doi.org/10.1080/01431160802665926.

White, M.A., Nemani, R.R., Thornton, P.E., Running, S.W., 2002. Satellite evidence of phenological differences between urbanized and rural areas of the eastern United States deciduous broadleaf forest. Ecosystems 5, 260–273. https://doi.org/10.1007/s10021-001-0070-8.

White, M., Thomton, P., Running, S., 1997. A continental responses phenology model climatic for monitoring variability vegetation to interannual. Glob Biogeochem Cycles 11, 217–234. https://doi.org/10.1029/97GB00330.

Yang, C., Deng, K., Peng, D., Jiang, L., Zhao, M., Liu, J., Qiu, X., 2022. Spatiotemporal Characteristics and Heterogeneity of Vegetation Phenology in the Yangtze River Delta, Remote Sensing.

Yao, R., Wang, L., Huang, X., Guo, X., Niu, Z., Liu, H., 2017. Investigation of urbanization effects on land surface phenology in Northeast China during 2001–2015. Remote Sens. (Basel) 9, 66. https://doi.org/10.3390/rs9010066.

Yu, L., Wang, J., Li, X., Li, C., Zhao, Y., Gong, P., 2014. A multi-resolution global land cover dataset through multisource data aggregation. Science China Earth Sciences 44, 1646-1660.doi: CNKI:SUN:JDXG.0.2014-10-005.

Zeng, L., Wardlow, B.D., Xiang, D., Hu, S., Li, D., 2020. A review of vegetation phenological metrics extraction using time-series, multispectral satellite data. Remote Sens. Environ. 237, 111511 https://doi.org/10.1016/j.rse.2019.111511.

Zhang, X., 2018. Land surface phenology: climate data record and real-time monitoring. In: Liang, S. (Ed.), Comprehensive Remote Sensing. Elsevier, Oxford, pp. 35–52.

Zhang, J., Chen, S., Wu, Z., Fu, Y.H., Environment, 2022. Review of vegetation phenology trends in China in a changing climate. 46, 829-845.

Zhang, X., Friedl, M.A., Schaaf, C.B., Strahler, A.H., Hodges, J.C.F., Gao, F., Reed, B.C., Huete, A., 2003. Monitoring vegetation phenology using MODIS. Remote Sens. Environ. 84, 471–475. https://doi.org/10.1016/S0034-4257(02)00135-9.

Zhang, X., Friedl, M.A., Schaaf, C.B., Strahler, A.H., Schneider, A., 2004. The footprint of urban climates on vegetation phenology. Geophys. Res. Lett. 31 (12), n/a–n/a.

Zhang, X., Friedl, M.A., Schaaf, C.B., 2006. Global vegetation phenology from Moderate Resolution Imaging Spectroradiometer (MODIS): Evaluation of global patterns and comparison with in situ measurements. J. Geophys. Res. Biogeo. 111 https://doi.org/10.1029/2006JG000217.

Zhang, W., Randall, M., Jensen, M.B., Brandt, M., Wang, Q., Fensholt, R., 2021. Socio-economic and climatic changes lead to contrasting global urban vegetation trends. Glob. Environ. Chang. 71, 102385 https://doi.org/10.1016/j.gloenvcha.2021.102385.

Zhao, L., Lee, X., Smith, R.B., Oleson, K., 2014. Strong contributions of local background climate to urban heat islands. Nature 511, 216–219. https://doi.org/10.1038/nature13462.

Zhou, D., Zhao, S., Liu, S., Zhang, L., Zhu, C., 2014. Surface urban heat island in China's 32 major cities: Spatial patterns and drivers. Remote Sens. Environ. 152, 51–61. https://doi.org/10.1016/j.rse.2014.05.017.

Zhou, D., Zhao, S., Zhang, L., Sun, G., Liu, Y., 2015. The footprint of urban heat island effect in China. Sci. Rep. 5, 1–11. https://doi.org/10.1038/srep11160.

Zhou, D., Zhang, L., Hao, L., Sun, G., Liu, Y., Zhu, C., 2016a. Spatiotemporal trends of urban heat island effect along the urban development intensity gradient in China. Sci. Total Environ. 544, 617–626. https://doi.org/10.1016/j.scitotenv.2015.11.168.

Zhou, D., Zhao, S., Zhang, L., Liu, S., 2016b. Remotely sensed assessment of urbanization effects on vegetation phenology in China's 32 major cities. Remote Sens. Environ. 176, 272–281. https://doi.org/10.1016/j.rse.2016.02.010.